

Singlet Oxygen Lifetime in Vitamin E Emulsion Depends on the Oil-Droplet Size

Keishi Ohara,* Takashi Origuchi, and Shin-ichi Nagaoka

Department of Chemistry, Faculty of Science, Ehime University, Matsuyama 790-8577

Received October 15, 2009; E-mail: ohara@chem.sci.ehime-u.ac.jp

The singlet oxygen ($^1O_2$) behavior in emulsions dispersing natural vitamin E (VE) (α-, β-, γ-, and δ-tocopherols) was investigated by measuring time-profiles of $^1O_2$ phosphorescence. The $^1O_2$ rise and decay dynamics noticeably reflected the existence of VE oil-droplets. The decay rate constant (k_d) in the α-tocopherol emulsion decreased with increase of VE concentration ([VE]), and became roughly constant in [VE] $\geq 5 \times 10^{-4}$ M. This k_d behavior correlated to the oil-droplet diameter measured by dynamic light scattering. The droplet diameter increased rapidly from 270 to 430 nm with increase of [VE], and reached the limit for dispersing in [VE] $\geq 5 \times 10^{-4}$ M. This result means that the $^1O_2$ surroundings became more hydrophobic with increase of droplet size. On the other hand, in the emulsions dispersing tocopherols other than α-tocopherol, the k_d values were roughly constant, indicating that the oil-droplets did not contribute to $^1O_2$ quenching. The droplet diameter in the δ-tocopherol emulsion was around 212–243 nm and was much smaller than that in the α-tocopherol emulsion. The peculiar results observed in the α-tocopherol emulsion should be due to the large hydrophobicity of α-tocopherol which has two methyl-groups neighboring the OH group.

An emulsion is a heterogenous system like a liquid or a cream which is a mixture of two or more liquids, such as water and oil, which do not mix naturally. For example, oil in water (o/w) emulsions are made by suspending numerous small oil-droplets with or without surfactants in water or water-base solvents.[1,2] Such emulsions are often found in natural or industrial materials, for example, serum, cytoplasm, drugs, cosmetics, foods, drinks, inks, paints, and photographic film systems. Emulsions are important and useful because they can deliver large amount of lipophilic functional compounds to cells and tissues of livings with water-base fluids. Hence, these inhomogeneous systems have often been used as a model for liposomes or cells in biological systems. From the industrial point of view, the emulsion is one of the best media to put effective and functional ingredients in water or alcohol base fluids or creams, as found in inks, cosmetics, and supplements.

Antioxidant behaviors in emulsions containing antioxidants are of great interest. For example, lipophilic antioxidants, such as carotenoids and vitamin E, or poorly water-soluble antioxidants, such as catechins, flavonoids, and other polyphenols, would be dispersed in emulsions. Such emulsions should have some antioxidant activity, but the emulsion, which contains oil-droplets, a bulk-phase, and the interfacial region between them, is too complicated to estimate its antioxidant efficiency. There are numerous kinetic and quantitative studies on this theme, but it has been difficult to investigate antioxidant processes in emulsions by any time-resolved spectroscopy because of the interference by opacity and photo-scattering of samples.[3–6] The direct investigation of emulsions using accurate time-resolved spectroscopy of the antioxidant processes versus the reactive-oxygen species (ROS), such as free-radicals and singlet oxygen ($^1O_2$), is very important and an attractive theme.

Vitamin E (VE) is a group of compounds having a 6-hydroxychroman moiety. VE is widely distributed in animals and plants, especially contained richly in plant oils, such as soy-bean oil. α-, β-, γ-, and δ-Tocopherols (Figure 1) are naturally occurring VE homologs with a 16-carbon isoprenoid side-chain at the 2-position.[5–14] These natural VEs are lipophilic and poorly water-soluble. VE is known as a biologically functional compound, for example, as an inhibitor of diseases, as a biomembrane stabilizer, and as an antioxidant against oxidative stress and ROS.[7–16] In biological systems, these natural tocopherols are believed to be located and function in hydrophobic environments, such as biomembranes. VE is also used extensively as an antioxidant or a medicinally functional additive in foods, drinks, supplements, cosmetics, and drugs.

Previously, we reported that a stable emulsion system dispersing α-tocopherol without surfactants could be made in 1:1 (v/v) ethanol/water mixed solvent (E/W).[17] In this emulsion system, there is no surfactant on the surface of oil-

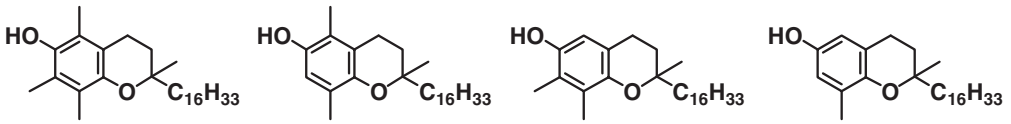

(a) α-Tocopherol (b) β-Tocopherol (c) γ-Tocopherol (d) δ-Tocopherol

Figure 1. Structures of α-, β-, γ-, and δ-tocopherols.

Published on the web February 26, 2010; doi:10.1246/bcsj.20090277

droplets. Our interest there was behaviors of this naked VE oil-droplet and the interface between the oil and the bulk solution phase with respect to $^1O_2$ dynamics in such inhomogeneous emulsion media. Singlet oxygen ($^1O_2$) is molecular oxygen in the electronically lowest excited $^1\Delta_g$ state.[18–22] $^1O_2$ is generated in chemical and biological systems through photosensitization by dye molecules. $^1O_2$ induces and accelerates oxidation of materials, and is thought to be an origin of photodegradation in plants and cancers in animals. Plants are believed to have protective compounds against $^1O_2$ generation, and some $^1O_2$ quenchers are actually used in cosmetics for skin care and in medicine, as well as UV protection materials. The investigation of $^1O_2$ dynamics in an emulsion might provide application and understanding of such systems.[17,23–26] The measurements of decay rates of $^1O_2$ phosphorescence around 1274 nm in the emulsion containing α-tocopherol gave a peculiar result that the decay rate decreased with increase of α-tocopherol concentration, although α-tocopherol should work as a good quencher. The result must come from formation of α-tocopherol droplets, which noticeably influences $^1O_2$ decay dynamics. It is known that the $^1O_2$ lifetime is very sensitive to its surroundings, and is relatively longer in hydrophobic media than in protic media.[20,27] Thus it is probable that $^1O_2$ phosphorescence occurred near the oil droplets and as a result the $^1O_2$ lifetime increased since the $^1O_2$ surroundings was hydrophobic. It was thought that the variation of the $^1O_2$ decay rate in the α-tocopherol emulsion was related to the size of the VE droplets; that is, the droplet size increased with increase of α-tocopherol concentration at low concentration ($<4 \times 10^{-4}$ M) and it became almost constant at high concentration ($>5 \times 10^{-4}$ M). For confirming this, further investigations are needed for $^1O_2$ dynamics and size distributions of oil-droplets in emulsions containing tocopherols.

The present study has been made to clarify $^1O_2$ dynamics in emulsion systems containing natural VEs (α-, β-, γ-, and δ-tocopherols) by measuring time-profiles of $^1O_2$ phosphorescence using single-photon-counting. Detection of $^1O_2$ ($^1\Delta_g$) phosphorescence around 1274 nm is the most accurate and reliable method for studying $^1O_2$ dynamics, especially when investigating opaque and scattering samples, such as the present emulsion systems.[17,23–31] Measurements by single-photon-counting used here can avoid occurrence of bimolecular self-quenching among $^1O_2$, and can also determine the formation rate of $^1O_2$ as well as the decay rate.[28] In order to clarify a relation between the change in $^1O_2$ dynamics and the oil-droplet formation, size distribution of oil-droplets contained in the VE emulsions has been measured by dynamic light scattering (DLS) with varying VE concentration ([VE]). From the results, the relation between oil-droplet formation and $^1O_2$ dynamics in the VE emulsions is discussed.

Experimental

α-, β-, γ-, and δ-Tocopherols were supplied from Eisai Co., Ltd. Rose bengal (RB) was commercially available reagent from TCI and was used as received. Ethanol (Wako) was dried and purified by distillation. Deionized water was treated with an ion-exchange column (Millipore Milli-Q). All sample solutions for $^1O_2$ phosphorescence measurements contained RB (2.0×10^{-4} M) as a photosensitizer. VE emulsion solutions were prepared in 1:1 (v/v) ethanol/water mixed solvent (E/W) by mixing an ethanol solution of each tocopherol with the same volume of deionized water. The sample solutions were handled under air-saturated conditions.

Procedures of $^1O_2$ phosphorescence measurements were the same as reported previously.[17,30] Spectra and time-evolutions of $^1O_2$ phosphorescence were measured at room temperature with a time-resolved near-infrared fluorescence spectrophotometer (Hamamatsu C-7990-01) operating in single-photon-counting mode. A DPSS Nd-YAG laser (CryLas FTSS355Q, SHG:532 nm, 14 kHz, FWHM 1 ns) was attenuated by an ND filter and used for photoexcitation. An IR700 sharp-cut filter was additionally used for cutting the emission of RB and second-order diffraction light. Laser excitation of the RB and O_2 containing sample generates $^1O_2$ through energy transfer (ET) from the lowest-excited triplet state of RB (^{3}RB*) to the ground state molecular oxygen ($^3O_2$, $^3\Sigma_g$) (Reaction 1).

$$^3\mathrm{RB}^* + {}^3\mathrm{O}_2 \xrightarrow{\mathrm{ET}} \mathrm{RB} + {}^1\mathrm{O}_2 \quad (1)$$
$$^1\mathrm{O}_2 \rightarrow {}^3\mathrm{O}_2 + h\nu \text{ (ca. 1274 nm)}$$

Apparent rise and decay rate-constants (k_r and k_d) for the $^1O_2$ phosphorescence at 1274 nm were determined by a least-squares fit of time-profile data subtracting the background counts to eq 2.[28,30]

$$I = I_0\{\exp(-k_d t) - \exp(-k_r t)\} \quad (2)$$

Size distribution of oil-droplets in emulsions was measured at 25 °C by a dynamic light scattering photometer (Otsuka Electronics, DLS-6000EW).

Results and Discussion

$^1O_2$ Quenching by Tocopherols in Ethanol. Figure 2a shows time profiles of $^1O_2$ phosphorescence at 1274 nm observed in ethanol in the absence of VE (solid line) and in the presence of α-tocopherol (circles, 7.02×10^{-4} M). In the absence of VE, the rate constant of $^1O_2$ decay was determined to be $k_0 = 6.49 \times 10^4\,s^{-1}$ ($^1O_2$ lifetime $\tau = 15.4\,\mu s$) as the natural decay rate constant in ethanol.[17,20,27] Addition of $^1O_2$ quencher such as tocopherols to the solution usually accelerates $^1O_2$ decay as shown in Figure 2a.[17,28–30] On the other hand, the rate of increase in $^1O_2$ phosphorescence was constant whether in the presence or in the absence of α-tocopherol. The reason for this is that the rise of $^1O_2$ phosphorescence is usually due to $^1O_2$ generation through photosensitization between ^{3}RB and ground state O_2. Thus, the rate of increase should be controlled by the diffusion and the oxygen concentration ([O_2]) in solutions.[28,30,32,33]

When $^1O_2$ quenching progresses through a bimolecular process between $^1O_2$ and a quencher (Q) (Reaction 3), the $^1O_2$ decay rate constant (k_d) is expressed as the following eq 4.[17,28–30]

$$^1\mathrm{O}_2 + \mathrm{Q} \xrightarrow{k_q} \text{Quenching products} \quad (3)$$
$$k_d = k_0 + k_q[\mathrm{Q}] \quad (4)$$

where k_0 and k_q are the natural decay rate constant of $^1O_2$ in the medium and the second-order rate constant of the $^1O_2$ quenching reaction by Q, respectively. The k_q value can be determined from a slope of the plot of k_d versus the concentration of Q ([Q]). Figure 2b shows plots of k_d values versus [VE] for α-, β-, γ-, and δ-tocopherols in ethanol. From the slope obtained for each tocopherol, the k_q values were determined to be 1.22×10^8, 1.38×10^8, 1.04×10^8, and

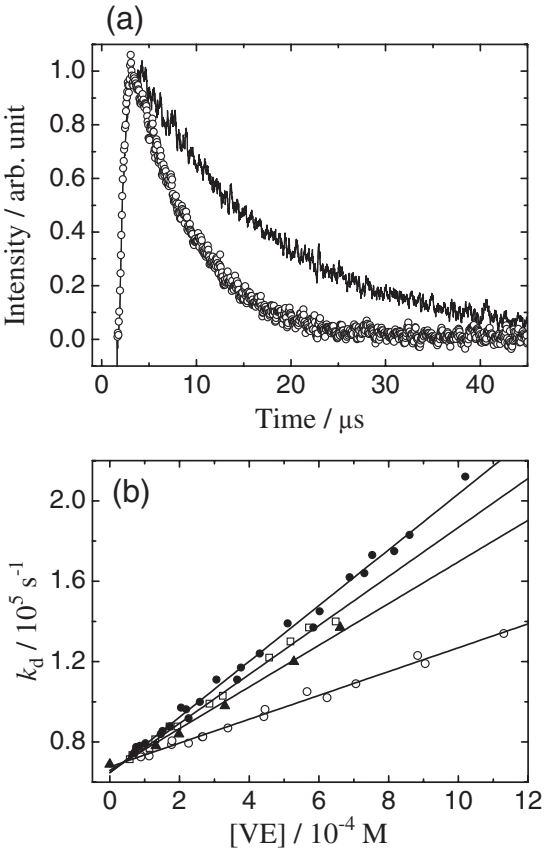

Figure 2. (a) Time-evolution of $^1O_2$ phosphorescence at 1274 nm in ethanol in the absence of VE (solid line) and in the presence of α-tocopherol (7.02×10^{-4} M, circle). High-frequency random noise was removed by a smoothing method. (b) Plots of k_d vs. [VE] obtained in ethanol for α-tocopherol (square, a part of data from Ref. 17), β-tocopherol (closed circle), γ-tocopherol (triangle), and δ-tocopherol (open circle).

5.93×10^7 M^{-1} s^{-1} for α-, β-, γ-, and δ-tocopherols, respectively (Table 1). These values are comparable to those in the literature.[13,20] The k_q value for natural tocopherols decreases in the order of β-tocopherol $\geq$ α-tocopherol > γ-tocopherol > δ-tocopherol. The same tendency was obtained for the k_q values measured in toluene by time-resolved EPR (Table 1). δ-Tocopherol has the smallest k_q value among these natural tocopherols, which is close to that of Trolox ($k_q = 5.17 \times 10^7$ M^{-1} s^{-1}).[30] $^1O_2$ quenching by tocopherols is considered to progress through an intermediate having partial charge-transfer character.[19,20,29,35] Therefore, the quenching rate should depend on the redox-potential of tocopherols (Table 1), and should be in the order of α-tocopherol > β-tocopherol $\approx$ γ-tocopherol > δ-tocopherol. The redox potential of γ-tocopherol is as large as that of β-tocopherol, but the k_q value of γ-tocopherol is smaller than that of β-tocopherol.[13,34] The redox potential of Trolox is much lower than that of δ-tocopherol and close to that of β-tocopherol, but the k_q value of Trolox is close to δ-tocopherol.[34] These discrepancies in the present results are not clear, but there must be another factor in $^1O_2$ quenching, for example steric factors or the solvation around the hydroxy group of tocopherols.

Table 1. k_q Values and Peak Oxidation Potentials (E_p vs. Ag/Ag^+) of Tocopherols

	$k_q/10^8$ M^{-1} s^{-1}			E_p/mV vs. Ag/Ag^{+} a)
Solvent:	Ethanol	E/W	Toluene[b)]	Acetonitrile
Sensitizer:	RB	RB	TPP	—
α-Tocopherol	1.22	—	1.03	490
β-Tocopherol	1.38	1.44	1.15	550
γ-Tocopherol	1.04	1.4	0.67	560
δ-Tocopherol	0.593	1.04	0.43	640
Trolox	0.517[c)]	—	—	530

a) Values from Ref. 34. b) Values measured by time-resolved EPR using tetraphenylporphine (TPP) as a photosensitizer (unpublished result). c) Value from Ref. 30.

Rise and Decay Rates of $^1O_2$ Phosphorescence in VE Emulsions. Figure 3a shows time-profiles of $^1O_2$ phosphorescence at 1274 nm in E/W in the absence of VE (solid line) and in the presence of α-tocopherol (circles, 4.58×10^{-4} M). The phosphorescence spectrum of $^1O_2$ in E/W was similar to that in ethanol.[17] From the time profile in the absence of VE, the rate constant of $^1O_2$ natural decay in E/W was determined to be $k_0 = 1.57 \times 10^5$ s^{-1} ($\tau = 6.37$ μs). The k_0 value is rather larger than that in ethanol, because, as is well known, $^1O_2$ decay is largely accelerated by the presence of H_2O.[18–20]

The E/W solution containing 4.58×10^{-4} M α-tocopherol was a white-clouded emulsion.[17] The time-profile of $^1O_2$ phosphorescence for this emulsion was absolutely different from that in ethanol. Both the formation and decay rates were certainly reduced from those in the absence of VE. This unusual behavior in time-evolution of $^1O_2$ phosphorescence must be related to the emulsion formation. $^1O_2$ formation and decay dynamics in the VE emulsions should be different from that in homogeneous solutions.

Figures 3b and 3c show plots of the decay rate constant (k_d) of $^1O_2$ phosphorescence measured in E/W against [VE] for α-, β-, γ-, and δ-tocopherols. The results in E/W did not give simple linear relationships between k_d and [VE], in contrast to those in ethanol (Figure 2b). In the case of α-tocopherol (Figure 3b), with increase of [VE], the k_d value was first almost constant in the range of [VE] = 0–1×10^{-4} M, decreased in [VE] = 1–4×10^{-4} M, and finally was scattered but roughly constant (ca. 9.5×10^4 s^{-1}) in [VE] $\geq 5 \times 10^{-4}$ M, as reported before.[17] On the other hand, in the cases of β-, γ-, and δ-tocopherols (Figure 3c), with increase of [VE], the k_d values increased almost linearly at low concentration ($\leq 4.0 \times 10^{-4}$ M), and became roughly constant and scattered at large concentration ($\geq 6.0 \times 10^{-4}$ M).

These nonlinear variations of k_d should come from the emulsion formation. For example, addition of over 1.2×10^{-4} M α-tocopherol (marked by the arrow in Figure 3b) led to a cloudy E/W solution.[17] The critical concentrations for generating the clouded emulsions (CEC) in E/W were estimated from optical absorption spectra to be 1.2×10^{-4}, 3.4×10^{-4}, 2.9×10^{-4}, and 5.0×10^{-4} M for α-, β-, γ-, and δ-tocopherols, respectively. The CEC value (1.2×10^{-4} M) of α-tocopherol is much smaller than those of the other tocopherols, because of the greater lipophilicity and lower solubility in E/W of

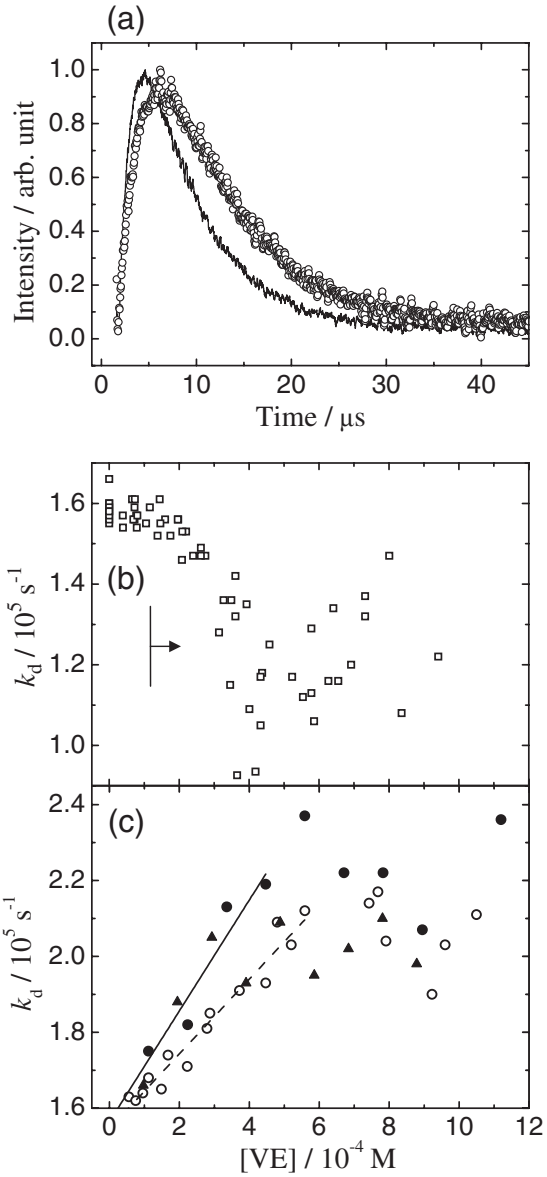

Figure 3. (a) Time-evolutions of $^1O_2$ phosphorescence at 1274 nm in E/W in the absence of VE (solid line) and in the presence of α-tocopherol (emulsion) (4.58×10^{-4} M, circle). (b) Plot of k_d vs. [VE] obtained in E/W for α-tocopherol (square). Emulsion formed in the range marked by the arrow. (c) Plots of k_d vs. [VE] obtained in E/W for β-tocopherol (closed circle), γ-tocopherol (triangle), and δ-tocopherol (open circle).

α-tocopherol. At larger concentration than CEC, numerous micro-size oil-droplets are formed and co-exist in the solution. The droplet size should be distributed in the range of 0.1–1 μm in the present white-clouded emulsion.[17]

At lower [VE] than CEC, the tocopherol solution was homogeneous and the $^1O_2$ quenching should progress through the reaction between $^1O_2$ and each tocopherol. From the linear relationship obtained between k_d and [VE] according to eq 4, the second-order rate constants k_q in E/W could be estimated to be 1.44×10^8, 1.4×10^8, and 1.04×10^8 M^{-1} s^{-1} for β-tocopherol ($\leq 3.5 \times 10^{-4}$ M), γ-tocopherol ($\leq 3.0 \times 10^{-4}$ M), and δ-tocopherol ($\leq 5.0 \times 10^{-4}$ M), respectively (Table 1). The value of γ-tocopherol has a large error coming from the scattered k_d data. The k_q value for α-tocopherol in E/W could not be determined because CEC for α-tocopherol was too small. The k_q values for β- and γ-tocopherols are very similar to each other, and are by 35% larger than that for δ-tocopherol. These k_q values in E/W are larger than those in ethanol (Table 1). Similar enlargement in k_q of tocopherols in water-containing solvents is described in the literature.[35,36] It might result from solvation effects or changes in the charge distribution around the OH of tocopherols. The acceleration of the reaction rate by H_2O addition was also observed in the free-radical scavenging by tocopherols and some polyphenols.[37]

In larger [VE] than CEC, the k_d values of β-, γ-, and δ-tocopherols became roughly constant and scattered. Such behaviors suggest that the k_d value is not controlled by $^1O_2$ quenching presented in eq 4. In [VE] > CEC, the oil-droplets increase with increase of [VE], and the VE concentration in the bulk phase would remain at saturated concentration. The constant k_d value in [VE] > CEC suggests that tocopherols in the oil-droplets scarcely contribute to $^1O_2$ quenching although the reactive OH group of tocopherol would be placed on the droplet surface. In these emulsion systems, since the $^1O_2$ quenching occurs mostly in the bulk solution phase, only the tocopherol fraction dissolved in the bulk solution should participate in $^1O_2$ quenching. As a result, the k_d values remain almost constant in the concentration range forming the emulsions.

On the other hand, the k_d behavior of α-tocopherol-containing E/W solution (Figure 3b) is unusual and different from those for the other tocopherols. The k_d value decreased with an increase of [VE] in the range of [VE] = 1–4 $\times 10^{-4}$ M, and became almost constant in [VE] $\geq 5 \times 10^{-4}$ M. This behavior of k_d should mainly be affected by the environment around $^1O_2$, because the $^1O_2$ lifetime is very sensitive to its surroundings, such as the solvents. In fact, the $^1O_2$ lifetime is relatively longer in hydrocarbons and aprotic solvents than in protic solvents.[20,27] We consider that $^1O_2$ phosphorescence occurs in the interface region between the bulk phase and the oil droplets in the α-tocopherol emulsion. If so, the increase in $^1O_2$ lifetime ($1/k_d$) can be explained, because the hydrophobicity (aprotic) of the oil-droplets makes the $^1O_2$ surroundings hydrophobic. In addition, the variation of k_d in the α-tocopherol emulsion might be related to the size of the VE droplets. Thus $^1O_2$ surroundings should become more hydrophobic with the increase of droplet size. In the α-tocopherol emulsion, the droplet size is thought to increase with increase of [VE] in [VE] = 1–4 $\times 10^{-4}$ M, and is thought to be almost constant in [VE] $\geq 5 \times 10^{-4}$ M. Compared with such change of the $^1O_2$ surroundings, the contribution of the oil-droplet in $^1O_2$ quenching was negligible, suggesting that the OH group of tocopherol in the oil-droplets scarcely contributed to $^1O_2$ quenching.

Figure 4 shows plots of the rise rate constant (k_r) of $^1O_2$ phosphorescence measured in E/W against [VE] for α-, β-, γ-, and δ-tocopherols. Here, for obtaining better results, the measurements for β-, γ-, and δ-tocopherols were carried out under O_2 saturated conditions. In the case of α-tocopherol

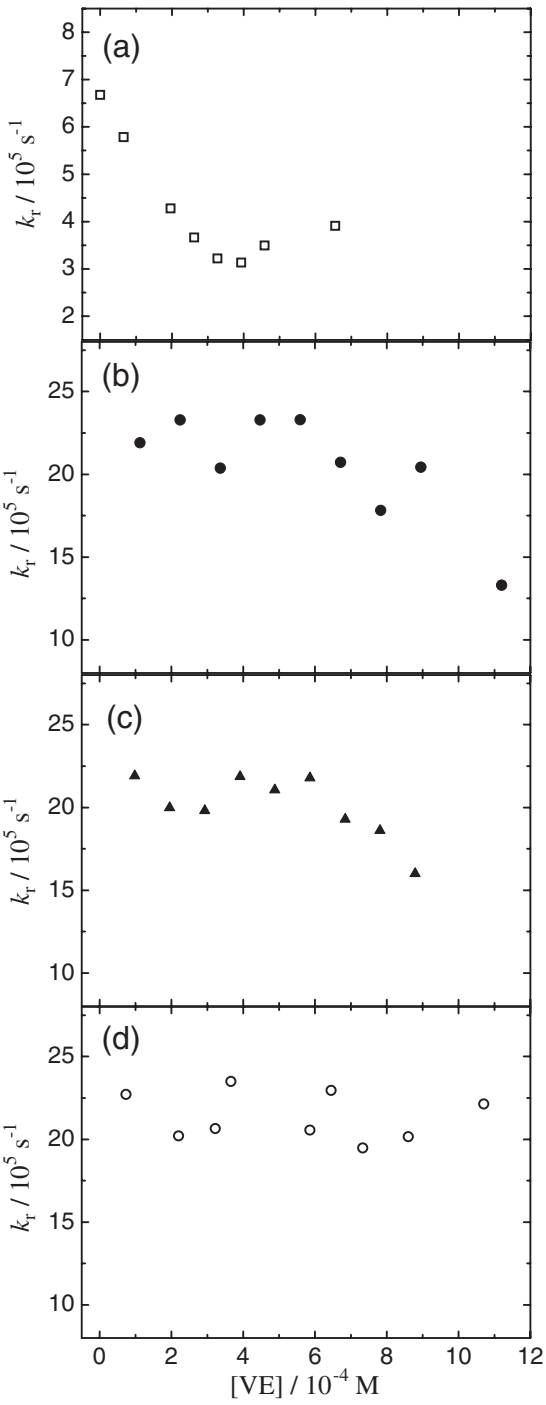

Figure 4. Plots of k_r vs. [VE] obtained in E/W for (a) α-tocopherol (square), (b) β-tocopherol (closed circle), (c) γ-tocopherol (triangle), and (d) δ-tocopherol (open circle).

(Figure 4a), the k_r value decreased with increase of [VE] and became almost constant (ca. $3.5 \times 10^4\,s^{-1}$) in the range of [VE] $\geq 4 \times 10^{-4}$ M. In the cases of β- and γ-tocopherols (Figures 4b and 4c), the k_r values were roughly constant in [VE] $\leq 6 \times 10^{-4}$ M and decreased gradually with increase of [VE] in [VE] $> 6 \times 10^{-4}$ M. On the other hand, the k_r value in the δ-tocopherol system (Figure 4d) was almost constant in [VE] $= 1$–11×10^{-4} M. As described above, in homogeneous solutions, the increase rate was usually constant whether with

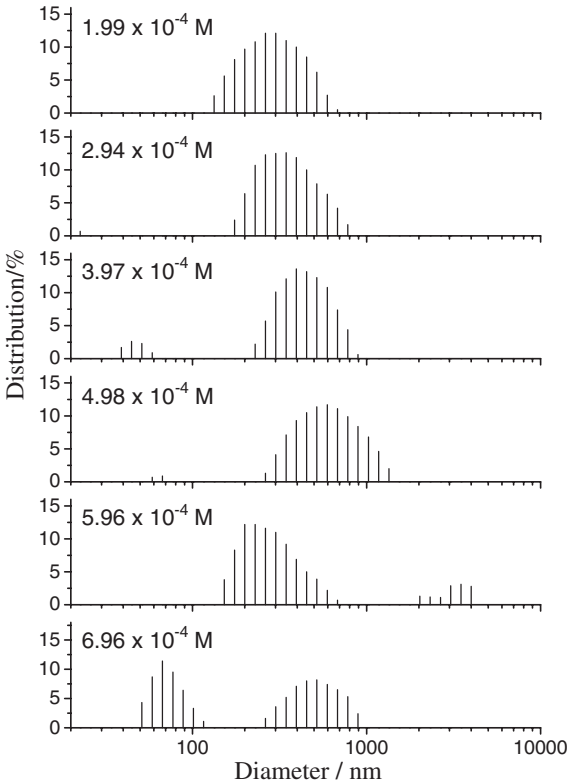

Figure 5. Concentration dependence of the distribution of the oil-droplet diameter measured for α-tocopherol emulsion by DLS at 25 °C.

or without $^1O_2$ quenchers (Figure 2a). On the contrary, a decrease in k_r was observed in the VE emulsion systems except for the δ-tocopherol system (Figure 4). The decrease of k_r should mean a decrease in the effective rate of $^1O_2$ generation through photosensitization progressing between O_2 and $^3RB^*$. Such a decrease of k_r usually originates from a decrease of O_2 concentration in solutions. In the present case, the decrease of k_r in the VE emulsions is considered to be caused by the oil-droplet formation. Probably, effective concentration of O_2 participating in the photosensitization was reduced by gathering O_2 around the oil-droplet surface, since O_2 might be more soluble in the hydrophobic region around the VE oil-droplets than in the E/W bulk phase.[17,38] As a result, the photosensitization rate between O_2 and $^3RB^*$ might be reduced from that in the homogeneous solution. The reduction of k_r with the oil-droplet formation was not observed for δ-tocopherol, suggesting that the region around the δ-tocopherol oil-droplets was less hydrophobic than those of the other tocopherols.

Size Distribution of Oil-Droplet in VE Emulsions. As described above, the [VE] dependence of k_d in the α-tocopherol emulsion is thought to relate to the size of the VE droplet. For confirming the above supposition, measurements of size distributions of the oil-droplets in the VE emulsions by DLS were tried.

Size distributions of the oil-droplets in the emulsions containing α- and δ-tocopherols at 25 °C are shown in Figures 5 and 6. The measurements for dilute CEC VE solutions ([VE] $< 1.2 \times 10^{-4}$ M for α-tocopherol, $< 5.0 \times 10^{-4}$ M for δ-tocopherol) were impossible because there was

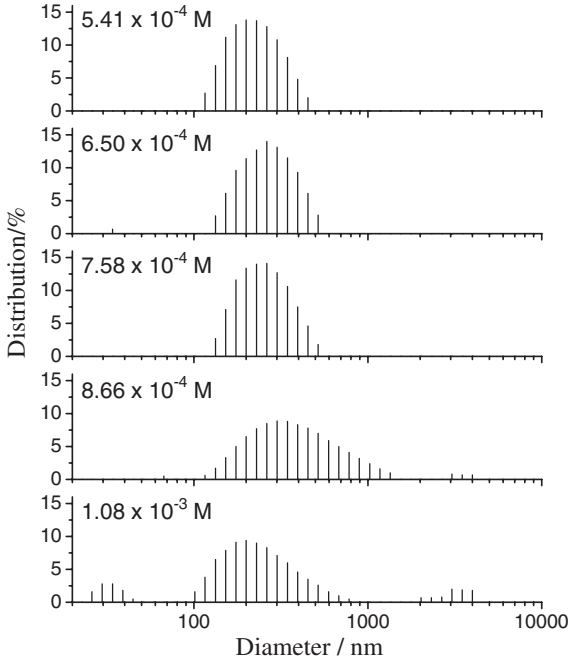

Figure 6. Concentration dependence of the distribution of the oil-droplet diameter measured for δ-tocopherol emulsion by DLS at 25 °C.

no measurable light-scattering in these samples. This fact suggests that tocopherol dissolved completely in these solutions. In the emulsion, the diameter distribution of the oil-droplet depends on [VE]. The droplet diameter in the α-tocopherol emulsion (Figure 5) was distributed in the range from 150 to 1000 nm. In [VE] $< 4.98 \times 10^{-4}$ M, the distribution showed a simple bell-shape close to the distribution of a monodisperse system, and the peak diameter in the distribution largely increased from 250 to 600 nm with increase of [VE]. In [VE] $> 5.96 \times 10^{-4}$ M, the diameter distribution was split into two peaks, indicating the change to a polydisperse system. The measurement for over 7×10^{-4} M α-tocopherol emulsion was impossible because of limitation of the DLS apparatus.

In the case of δ-tocopherol emulsion (Figure 6), the droplet diameter was distributed in the range from 100 to 1000 nm. In [VE] $< 7.58 \times 10^{-4}$ M, the distribution was also close to monodisperse, and the peak diameter in the distribution slightly increased from 200 to 250 nm with increase of [VE]. In [VE] $= 8.66 \times 10^{-4}$ M, the dispersion of the diameter distribution was enlarged, and double or triple distribution peaks appeared in [VE] $= 1.08 \times 10^{-3}$ M, indicating the change to a polydisperse.

Figure 7 shows plots of the mean values of the droplet-diameter in these VE emulsions against [VE]. In the case of the α-tocopherol emulsion, the mean diameter increased rapidly from 270 to 430 nm with increase of [VE] in the range of 1.99–6.96×10^{-4} M. In [VE] $< 4.0 \times 10^{-4}$ M, the diameter distribution was stable and the errors in the mean values were very small. However, the errors in [VE] $> 5.96 \times 10^{-4}$ M were very large, coming from the fact that the diameter distribution was unstable and split into plural peaks. In the case of δ-tocopherol emulsion, the mean diameter increased gradually from 212 to 243 nm with increase of [VE] in 5.41×10^{-4}–7.58×10^{-3} M, and decreased in [VE] $= 8.66 \times 10^{-4}$–1.08×10^{-3} M. The

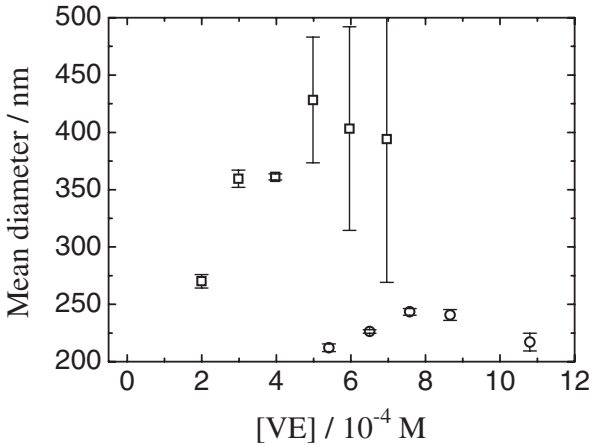

Figure 7. Mean-values of the oil-droplet diameter in α-tocopherol (square) and γ-tocopherol (circle) emulsions (Error bars show standard error of three experiments.).

errors in the mean diameter values were very small in 5.41×10^{-4}–7.58×10^{-3} M, and slightly larger in [VE] $= 8.66 \times 10^{-4}$–1.08×10^{-3} M. The result can also be explained by the change in distribution as well as in the case of the α-tocopherol emulsion.

$^1O_2$ Dynamics in VE Emulsion Depend on the Oil-Droplet Size. The results of the diameter distributions of oil-droplets were almost consistent with our interpretation on the k_d behavior. In the α-tocopherol emulsions, the increase of [VE] ($1–5 \times 10^{-4}$ M) induced the increase of the oil-droplet diameter, and simultaneously, induced the decrease in k_d. This means that $^1O_2$ surroundings became more hydrophobic with the increase of the droplet size. When the droplet size reached the limit for dispersing in [VE] $\geq 5 \times 10^{-4}$ M, the k_d value became constant, which means that the environment around $^1O_2$ became steady there although the number of droplets still increased with increase of [VE]. The fact that the k_d values were scattered in [VE] $\geq 6 \times 10^{-4}$ M is also consistent with the scatter of the diameter there. The relation between k_d and the oil-droplet diameter actually supports the following explanation of the $^1O_2$ dynamics. (1) $^1O_2$ phosphorescence in the VE emulsions occurred in the interface region around the oil-droplets where the environment was more hydrophobic than the bulk solution phase consisting of E/W. Therefore, the $^1O_2$ lifetime increased with the emulsion formation since the $^1O_2$ surroundings became hydrophobic. (2) The increase of the oil-droplet size made the interface region around the droplet more hydrophobic. (3) Tocopherols in the oil-droplet scarcely contribute to $^1O_2$ quenching although the OH group of tocopherol is thought to locate on the droplet surface. According to this interpretation, both fast and slow decay components related to the $^1O_2$ dynamics in the E/W bulk phase and that around the oil droplet should be observed. However, all the time-profile data could be fitted to eq 4, i.e., the decay curve was a single exponential curve. Similar phenomena were reported in the micelle and liposome systems.[39–41] This fact can be explained in the following way. The amount of $^1O_2$ around the oil droplets might be relatively larger than that in the bulk phase, because molecular oxygen is more soluble in the hydrophobic media than in E/W.[17,38] As a result, the decay

dynamics near the VE oil droplet appears more clearly than that of the bulk phase. Another explanation is possible from the distribution equilibrium of $^1O_2$ between hydrophobic and hydrophilic regions. $^1O_2$ can diffuse between the droplet surface and the bulk phase in its lifetime. There, the apparent $^1O_2$ decay should be a single exponential whose rate constant was controlled by the equilibrium constant and the $^1O_2$ lifetimes in the oil phase and in the bulk phase, as described in the literature.[23,39,40]

On the other hand, the decrease of k_d was not observed in β-, γ-, and δ-tocopherol emulsions. One reason for this might be that the oil-droplet size was too small to have an influence on the $^1O_2$ dynamics. Actually, in the δ-tocopherol emulsion, although the diameter slightly increased in the range of [VE] = 5.4–7.6 × 10^{-4} M, k_d was almost constant there. The mean diameter was 1/2–2/3 of that in the α-tocopherol emulsion, and the increase in the diameter was small. Another reason might be the difference in the interface properties around the droplet among these tocopherols. The interface region around the droplet of β-, γ-, and δ-tocopherols is thought to be less hydrophobic than that of the α-tocopherol droplet. It might lead to merely small increase in $^1O_2$ lifetime.

Among the natural tocopherols, only α-tocopherol showed notable and specific $^1O_2$ dynamics in the emulsion originating from the oil-droplet formation. One reason is thought to be that rather large droplets of α-tocopherol can be dispersed more stably in E/W than those of the other tocopherols. And also the surface of the α-tocopherol droplets is sufficiently hydrophobic as to gather $^1O_2$ or O_2 there and to increase $^1O_2$ lifetime. The structures of these natural tocopherols are different from each other in the number of methyl groups neighboring the phenolic OH on the chroman moiety. This structural difference should cause the difference in the size and surface properties of the oil-droplets. In the present tocopherol emulsions, the lipophilic alkyl-chain "tail" of tocopherols is hidden inside the droplet and the hydrophilic OH group "head" on the chroman moiety is in contact with the E/W bulk phase outside the droplet, as with colloids or o/w micelles. Compared with the other tocopherols, the oil-droplet surface is rather hydrophobic in the case of α-tocopherol which has two methyl groups protecting the OH group. This structural feature also makes the interfacial tension of the oil droplets versus the bulk phase large enough to stabilize the large size droplets.

The k_d value in the α-tocopherol emulsion seems to be affected by the surface area of the included droplets. On the other hand, from the fact that the k_d value became constant in [VE] ≥ 5 × 10^{-4} M, total surface area of the droplets in the emulsion is not thought to be essential for the k_d behavior because the total surface area should increase with increase of [VE]. Figure 8 shows plots of reciprocals of the surface area (S^{-1}) calculated from the mean diameter of oil-droplet vs. [VE] together with the plots of k_d for α-tocopherol in E/W vs. [VE]. The variation in k_d agrees with that of S^{-1}. The larger S, the more hydrophobic the surface of the oil-droplets would become.

Conclusion

The present study was made of $^1O_2$ behavior in emulsion systems dispersing natural VE by measuring time-profiles of $^1O_2$ phosphorescence using single-photon-counting. The k_d value in the α-tocopherol emulsion decreased with increase of [VE] in the range of [VE] = 1–4 × 10^{-4} M, and was scattered but roughly constant in [VE] ≥ 5 × 10^{-4} M. This k_d behavior correlated to the oil-droplet diameter estimated by the DLS measurements. The mean diameter increased rapidly from 270 to 430 nm with increase of [VE] in 1.99–4.98 × 10^{-4} M, and reached the limit for dispersing in [VE] ≥ 5 × 10^{-4} M. The increase of the oil-droplet diameter caused the decrease in k_d, simultaneously. This means that $^1O_2$ surroundings become more hydrophobic with the increase of the droplet size. On the other hand, in the emulsions of the other tocopherols, the k_d values were roughly constant. The result indicates that the oil-droplets generated in the emulsions do not contribute to $^1O_2$ quenching and would keep effective VE concentration saturating in the bulk phase. The mean diameter of the droplets in the δ-tocopherol emulsion was around 212–243 nm and was much smaller than that in the α-tocopherol emulsion. Thus, the $^1O_2$ formation and decay dynamics noticeably reflects the formation of the oil droplets, especially in the α-tocopherol emulsion. α-Tocopherol showed the peculiar behaviors on k_d and the oil-droplet diameter, which were quite different from those of the other natural tocopherols. The difference should be due to the large hydrophobicity of α-tocopherol which has two methyl groups neighboring the OH group on the chroman moiety.

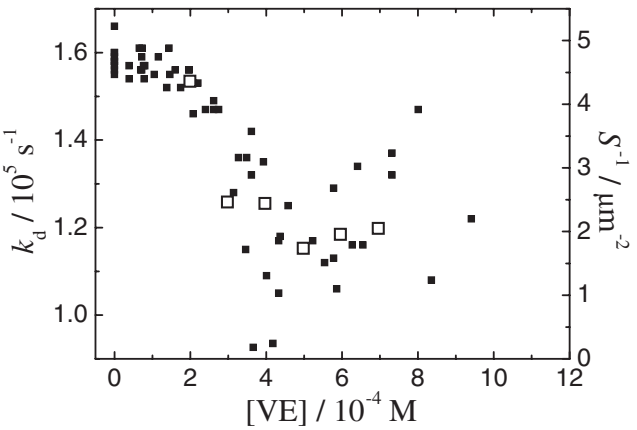

Figure 8. Plots of k_d (closed square) and reciprocal of the oil-droplet surface area (S^{-1}) (open square) vs. [VE] for the α-tocopherol emulsion.

We thank Professor Keiichi Kato of Ehime University for his kind help in DLS measurements. We also thank Eisai Co., Ltd. for the gift of α-, β-, γ-, and δ-tocopherols. This work was supported by Grant-in-Aid for Scientific Research C (No. 19550019) from the Japan Society for the Promotion of Science (JSPS). The apparatus (C-7990-01) was supplied by financial-support for instruments for scientific research from Ehime University.

References

1 B. K. Paul, S. P. Moulik, *Curr. Sci.* **2001**, *80*, 990.

2 B. K. Paul, S. P. Moulik, *J. Dispersion Sci. Technol.* **1997**, *18*, 301.

3 L. S. Romsted, J. Zhang, *J. Agric. Food Chem.* **2002**, *50*, 3328.

4 E. N. Frankel, S.-W. Huang, J. Kanner, J. B. German, *J. Agric. Food Chem.* **1994**, *42*, 1054.
5 S.-W. Huang, E. N. Frankel, J. B. German, *J. Agric. Food Chem.* **1994**, *42*, 2108.
6 S.-W. Huang, E. N. Frankel, K. Schwarz, J. B. German, *J. Agric. Food Chem.* **1996**, *44*, 2496.
7 G. W. Burton, T. Doba, E. J. Gabe, L. Hughes, F. L. Lee, L. Prasad, K. U. Ingold, *J. Am. Chem. Soc.* **1985**, *107*, 7053.
8 M. Mino, H. Nakamura, A. T. Diplock, H. J. Kayden, *Vitamin E*, Japan Scientific Society Press, Tokyo, **1993**.
9 G. W. Burton, K. U. Ingold, *Acc. Chem. Res.* **1986**, *19*, 194.
10 L. R. C. Barclay, *Can. J. Chem.* **1993**, *71*, 1.
11 K. Mukai, in *Vitamin E in Health and Diseases*, ed. by L. Packer, J. Fuchs, Macel Dekker, New York, **1992**.
12 E. Niki, *Chem. Phys. Lipids* **1987**, *44*, 227.
13 K. Mukai, K. Daifuku, K. Okabe, T. Tanigaki, K. Inoue, *J. Org. Chem.* **1991**, *56*, 4188.
14 S.-W. Huang, A. Hopia, K. Schwarz, E. N. Frankel, J. B. German, *J. Agric. Food Chem.* **1996**, *44*, 444.
15 A. Azzi, *Free Radical. Biol. Med.* **2007**, *43*, 16.
16 M. G. Traber, J. Atkinson, *Free Radical. Biol. Med.* **2007**, *43*, 4.
17 K. Ohara, T. Origuchi, K. Kawanishi, S. Nagaoka, *Bull. Chem. Soc. Jpn.* **2008**, *81*, 345.
18 A. A. Frimer, *Singlet O_2*, CRC Press, Boca Raton, FL, **1985**, Vols. I–IV.
19 C. Schweitzer, R. Schmidt, *Chem. Rev.* **2003**, *103*, 1685.
20 F. Wilkinson, W. P. Helman, A. B. Ross, *J. Phys. Chem. Ref. Data* **1995**, *24*, 663.
21 C. Triantaphylidès, M. Havaux, *Trends Plant Sci.* **2009**, *14*, 219.
22 M. J. Davies, *Biochem. Biophys. Res. Commun.* **2003**, *305*, 761.
23 L. A. Martinez, C. G. Martínez, B. B. Klopotek, J. Lang, A. Neuner, A. M. Braun, E. Oliveros, *J. Photochem. Photobiol., B* **2000**, *58*, 94.
24 S. Oelckers, T. Ziegler, I. Michler, B. Röder, *J. Photochem. Photobiol., B* **1999**, *53*, 121.
25 A. Cantrell, D. J. McGarvey, T. G. Truscott, F. Rancan, F. Böhm, *Arch. Biochem. Biophys.* **2003**, *412*, 47.
26 J. Baier, M. Maier, R. Engl, M. Landthaler, W. Bäumler, *J. Phys. Chem. B* **2005**, *109*, 3041.
27 O. Shimizu, J. Watanabe, K. Imakubo, S. Naito, *Chem. Lett.* **1999**, 67.
28 A. Jiménez-Banzo, X. Ragàs, P. Kapusta, S. Nonell, *Photochem. Photobiol. Sci.* **2008**, *7*, 1003.
29 S. Nagaoka, A. Fujii, M. Hino, M. Takemoto, M. Yasuda, M. Mishima, K. Ohara, A. Masumoto, H. Uno, U. Nagashima, *J. Phys. Chem. B* **2007**, *111*, 13116.
30 K. Ohara, K. Kikuchi, T. Origuchi, S. Nagaoka, *J. Photochem. Photobiol., B* **2009**, *97*, 132.
31 M. A. Rodgers, *Photochem. Photobiol.* **1983**, *37*, 99.
32 J. Baier, T. Maisch, J. Regensburger, M. Loibl, R. Vasold, W. Bäumler, *J. Biomed. Opt.* **2007**, *12*, 064008.
33 J. Baier, T. Fuβ, C. Pöllmann, C. Wiesmann, K. Pindl, R. Engl, D. Baumer, M. Maier, M. Landthaler, W. Bäumler, *J. Photochem. Photobiol., B* **2007**, *87*, 163.
34 A. Mitarai, A. Ouchi, K. Mukai, A. Tokunaga, K. Mukai, K. Abe, *J. Agric. Food Chem.* **2008**, *56*, 84.
35 R. H. Bisby, C. G. Morgan, I. Hamblett, A. A. Gorman, *J. Phys. Chem. A* **1999**, *103*, 7454.
36 S. Nonell, L. Moncayo, F. Trull, F. Amat-Guerri, E. A. Lissi, A. T. Soltermann, S. Criado, N. A. García, *J. Photochem. Photobiol., B* **1995**, *29*, 157.
37 K. Mukai, Y. Kanesaki, Y. Egawa, S. Nagaoka, in *Phytochemicals and Phytopharmaceuticals*, ed. by F. Shahidi, C.-T. Ho, AOCS Press, Champaign, **2000**.
38 S. L. Murov, *Handbook of Photochemistry*, Macel Dekker, New York, **1973**.
39 P. C. Lee, M. A. J. Rodgers, *J. Phys. Chem.* **1983**, *87*, 4894.
40 M. A. J. Rodgers, P. C. Lee, *J. Phys. Chem.* **1984**, *88*, 3480.
41 A. Molnár, R. Dědic, A. Svoboda, J. Hála, *J. Mol. Struct.* **2007**, *834–836*, 488.